PROTEINS
STRUCTURE ■ FUNCTION ■ BIOINFORMATICS

STRUCTURE NOTE

The structure of a shellfish specific GST class glutathione *S*-transferase from Antarctic bivalve *Laternula elliptica* reveals novel active site architecture

Ae Kyung Park,[1] Jin Ho Moon,[2] Eun Hyuk Jang,[1] Hyun Park,[3] In Young Ahn,[3] Ki Seog Lee,[4]* and Young Min Chi[1]*

[1] Division of Biotechnology, College of Life Sciences, Korea University, Seoul 136-713, Republic of Korea

[2] Institute of Life Sciences and Natural Resources, Korea University, Seoul 136-713, Republic of Korea

[3] Korea Polar Research Institute, Korea Ocean Research and Development Institute, Songdo-Dong 7-50, Yeonsu-Gu, Incheon 406-840, Republic of Korea

[4] Department of Clinical Laboratory Science, College of Health Sciences, Catholic University of Pusan, Busan 609-757, Republic of Korea

ABSTRACT

Glutathione-S-transferases have been identified in all the living species examined so far, yet little is known about their function in marine organisms. In a previous report, the recently identified GST from Antarctic bivalve *Laternula elliptica* (LeGST) was classified into the rho class GST, but there are several unique features of LeGST that may justify reclassification, which could represent specific shellfish GSTs. Here, we determined the crystal structure of LeGST, which is a shellfish specific class of GST. The structural analysis showed that the relatively open and wide hydrophobic H-site of the LeGST allows this GST to accommodate various substrates. These results suggest that the H-site of LeGST may be the result of adaptation to their environments as sedentary organisms.

Proteins 2013; 81:531–537.

INTRODUCTION

Glutathione *S*-transferases (GSTs, EC. 2.5.1.18) are a family of multi-functional enzymes that play a crucial role in phase II of enzymatic detoxification and excretion of harmful physiological and xenobiotic eletrophilic compounds.[1] They catalyze the addition of glutathione (GSH) to various substrates that have electrophilic functional groups, including hydrocarbons, organochlorine insecticides, and PCBs (polychlorinated biphenyls).[2,3] The produced GSH adducts have increased solubility in water and are subsequently degraded to mercapturates by enzyme reactions, and excreted.[4,5] GSTs are also involved in a wide range of biological processes. They play an important role in protecting the cells from the harmful effects of oxidative stress and have been implicated in various biosynthetic pathways.[6] Some GSTs are capable of binding to a large number of endogenous and exogenous compounds noncatalytically.[7]

Additional Supporting Information may be found in the online version of this article.

Grant sponsor: Korea Polar Research Institute (KOPRI); Grant number: PE10040.
*Correspondence to: Ki Seog Lee, Department of Clinical Laboratory, Science, College of Health Sciences, Catholic University of Pusan, Busan, 609-757, Republic of Korea. E-mail : kslee@cup.ac.kr and Young Min Chi, Division of Biotechnology, College of Life Sciences, Korea University, Seoul 136-713, Republic of Korea. E-mail: ezeg@korea.ac.kr
Received 22 June 2012; Revised 9 October 2012; Accepted 11 October 2012
Published online 14 November 2012 in Wiley Online Library (wileyonlinelibrary.com).
DOI: 10.1002/prot.24208

GSTs from a variety of organisms have been identified and characterized. Mammalian GSTs, which exist in the cytosol and form homodimers or heterodimers, have been particularly well characterized. In addition, through studies on nonmammalian species, novel classes of GSTs have been indentified in bacteria, plants, and insects. On the other hand, there is no standard of classification to categorize the GSTs from marine organisms. On the basis of the classification criteria of mammalian GSTs, marine GSTs are categorized into alpha, mu, pi, sigma, and theta classes; however, certain marine GSTs may belong to different classes when distinct characteristics are considered. The rho class GST is a representative class compared with other GSTs. Since the rho class GST, which is specific for fish, was identified in *Pagrus major*,[8] many other GSTs from marine organisms have also been classified into the rho class GST. A recently identified GST from Antarctic bivalve *Laternula elliptica* (LeGST) was also classified into the rho class in previous reports.[9]

L. elliptica is an important organism in the Antarctic food chain, and plays a role in monitoring environmental pollutants, such as PCBs, which are major persistent organic pollutants (POPs).[10] GSTs are more interesting biomarkers compared with other candidates currently under investigation. Changes in GST activity and transcriptional induction in response to PCB exposure have been investigated in several aquatic mollusks.[11–15] In addition, bivalve mollusks are able to bioaccumulate environmental pollutants; thus, they have been widely used as indicator species in marine environmental assessments.[9] Therefore, the LeGST holds great promise for use as an effective biomarker regarding environmental pollutants in Antarctica.

Despite the fact that LeGST was classified into the rho class GST in previous reports, there are several reasons for reconsidering this classification. Analyses of multiple sequence alignments, evolutionary tree, substrate specificity, and three-dimensional structure suggested that LeGST should be either categorized in a different group of GST from the rho class GST or reclassified into a new marine organism specific GST class. The new class GST consists of GSTs from marine sedentary organisms, including various types of shellfish, which is unlike the rho class GSTs that have been mainly identified in fish.[16] The shellfish specific GSTs have evolved to reduce the effects of any toxic xenobiotic compounds, resulting in a balanced substrate specificity without preference for certain substrates. This adaptation to their environment may be one reason to reclassify LeGST into a new class of GST, and further emphasizes that classification of GST should include information on their substrate specificity and three-dimensional structure. However, currently, there is no structural information on GSTs from marine organisms.

In this report, we determined the high-resolution crystal structure of LeGST from a marine organism, which is a shellfish specific class of GST. Moreover, the results of this study provides more detailed information on the first structure of a marine specific GST as well as differences between this GST and other GST classes. The crystal structure of LeGST contained unique features compared with other previously known structures, especially the hydrophobic substrates binding site (H-site), which is formed by a kinked α4 helix and extended C-terminal tail. These two components of the H-site could be used to explain how LeGST was utilized to allow these sedentary organisms to survive in polluted environments.

MATERIALS AND METHODS

Recombinant protein expression, purification, and crystallization

The heterologous expression of LeGST in *Escherichia coli*, purification and crystallization were performed as previously described.[17] Briefly, the crystals of apo-LeGST and LeGST-GSH complex were obtained by the sitting-drop vapor diffusion method at 22°C; each drop was made up of a 4 μL protein solution (10 mg/mL) [20 m*M* Tris-HCl, pH 7.9, 200 m*M* NaCl, 2 m*M* DTT] and a 4 μL reservoir solution [6% Tacsimate, pH 8.0 and 26% (*w*/*v*) polyethylene glycol 3350], and was equilibrated over a 500 μL reservoir solution. For cocrystallization, the protein solution was mixed with GSH in a 1:1 molar ratio. For multiple-wavelength anomalous dispersion (MAD) phasing, the selenomethionine-substituted protein was cultured by growing the expression plasmid in *E. coli* B834 (DE3), using the M9 cell culture medium containing extra amino acids. The SeMet-substituted protein was purified by the same procedure used for native protein except for the presence of 10 m*M* β-mercaptoethanol in all buffers used during the purification steps for protection from oxidizing of selenomethionyl protein. The crystals of SeMet-substitute LeGST were grown by the sitting-drop vapor diffusion method under the same condition of apo-crystal. Suitable-sized crystals were obtained within 3 days and were used for X-ray diffraction.

Data collection and processing

For cryogenic experiments, crystals were soaked in mother liquor plus 25% (*v*/*v*) ethylene glycol and flash-frozen in a liquid-nitrogen stream. The diffraction data set of SeMet-substituted crystal were collected on beamline 6C at the Pohang Light Source (Pohang, South Korea) using an ADSC Quantum 210 CCD detector. For the SeMet crystal, a total of 360 frames were collected with an oscillation range of 1°. Diffraction data were collected at single wavelength corresponding to the peak (λ = 0.9798 Å) of a selenium *K*-edge absorption profile, and were indexed, integrated and scaled by using

Table I
Data Collection and Refinement Statistics

Data collection	SeMet	Native	GSH-complex
Space group		C2	
Wavelength (Å)	0.97968	1.0000	1.0000
Cell dimension (Å)	a = 89.60, b = 56.92, c = 54.98, β = 123.16°	a = 89.66, b = 59.27, c = 55.45, β = 124.52°	a = 90.39, b = 57.62, c = 545.45, β = 123.83°
Resolution range (Å)	50.0–2.5 (2.59–2.50)	50.0–2.0 (2.00–2.07)	50.0–2.2 (2.20–2.28)
Total reflections	38,217	81,229	57,369
Unique reflections	7,633	15,882	11,607
Completeness (%)	93.4 (85.1)	96.0 (83.7)	95.9 (86.6)
R_{merge}[a] (%)	9.3 (13.9)	7.3 (19.3)	13.3 (24.3)
Redundancy	5.0 (3.2)	5.1 (3.0)	4.9 (3.9)
$<I/\sigma(I)>$	15.3 (3.73)	35.6 (5.1)	19.8 (4.2)
Refimenet			
	Native		GSH-complex
Space group	C2		
Resolution range (Å)	50.5–2.0		50.0–2.2
R/R_{free}[b] (%)	21.1/24.7		21.4/26.8
No. of amino acid residues (B-factor, Å^2)	219 (39.2)		219 (30.9)
No. of waters (B-factor, Å^2)	109 (41.3)		130 (33.1)
RMS deviation of			
Bond length (Å)	0.007		0.008
Bond angle (°)	1.3		1.4
In Ramachandran plot			
Most favored (%)	88.7		91.8
Additionally allowed (%)	11.3		8.2

Data collection values in parentheses are for the highest resolution shell.
[a] $R_{merge} = \sum_h \sum_i |I(h)_i - <I(h)>| / \sum_h \sum_i I(h)_i$ is the intensity of reflection h, $\sum_h$ is the sum over all reflections, and $\sum_i$ is the sum over i measurement of reflection h.
[b] $R = \sum ||F_{obs}| - |F_{calc}|| / \sum |F_{obs}|$, where R_{free} is calculated for a randomly chosen 5% of reflections, which were not used for structure refinement.

HKL2000.[18] The data-collection statistics are summarized in Table I.

Structure solution and refinement

The structure of LeGST was determined by the single-wavelength anomalous dispersion (SAD) method using a SeMet-substituted crystal. The location of selenium positions, initial phase calculations, phase improvement through density modification, and initial maps were calculated using the PHENIX program suite.[19] A total of 6 Se sites in the asymmetric unit were determined, and the overall figure of merit (FOM) was improved to 0.56 and automatically built 175 residues out of 219 residues for one asymmetric unit. Building and refinement were performed using cycles of model building with Coot[20] and refinement with PHENIX.[19] At this stage, the use of a higher-resolution native dataset was continued for further refinement. After several cycles of model building, simulated annealing, positional refinement, and individual B-factor refinement, the final R_{cryst} and R_{free} values were 19.1 % and 23.5 %, respectively. The final model contains one protein monomer 219 amino acids residues and 108 water molecules. Subsequently, the resulting structure of ligand-free LeGST was used as a model for the GSH-bound structure. The density for GSH in the G-site was very interpretable, and then the ligand was fitted in the right position. The stereochemical qualities for all of the final models as assessed by PROCHECK[21] were excellent. The refinement statistics are summarized in Table I.

RESULTS AND DISCUSSION

Overall structure and identification of new class of GST

The crystal structure of the LeGST was a monomer consisting of 219 residues, which formed a dimer in the crystallographic 2-fold rotation. Each monomer is made up of two domains; a small thioredoxin-like N-terminal domain (residues 5–91) and a larger helical C-terminal domain (residues 92–223). The N-terminal domain consists of three α-helices and four β-strands and the C-terminal domain consisted of five α-helices. Although the overall fold of LeGST adopts a similar conformation as other GST classes, there are two distinct structural features in LeGST that distinguished it from other GST families. One feature is the relatively more open and wide H-site of the LeGST, which allows access to a broad range of substrates, regardless of substrate size. The other feature is observed at the dimer interface, which consists of a hydrophobic environment around a two-fold axis and a modified lock-and-key motif.

LeGST shares low sequence similarity with other GST classes, which have been structurally identified in

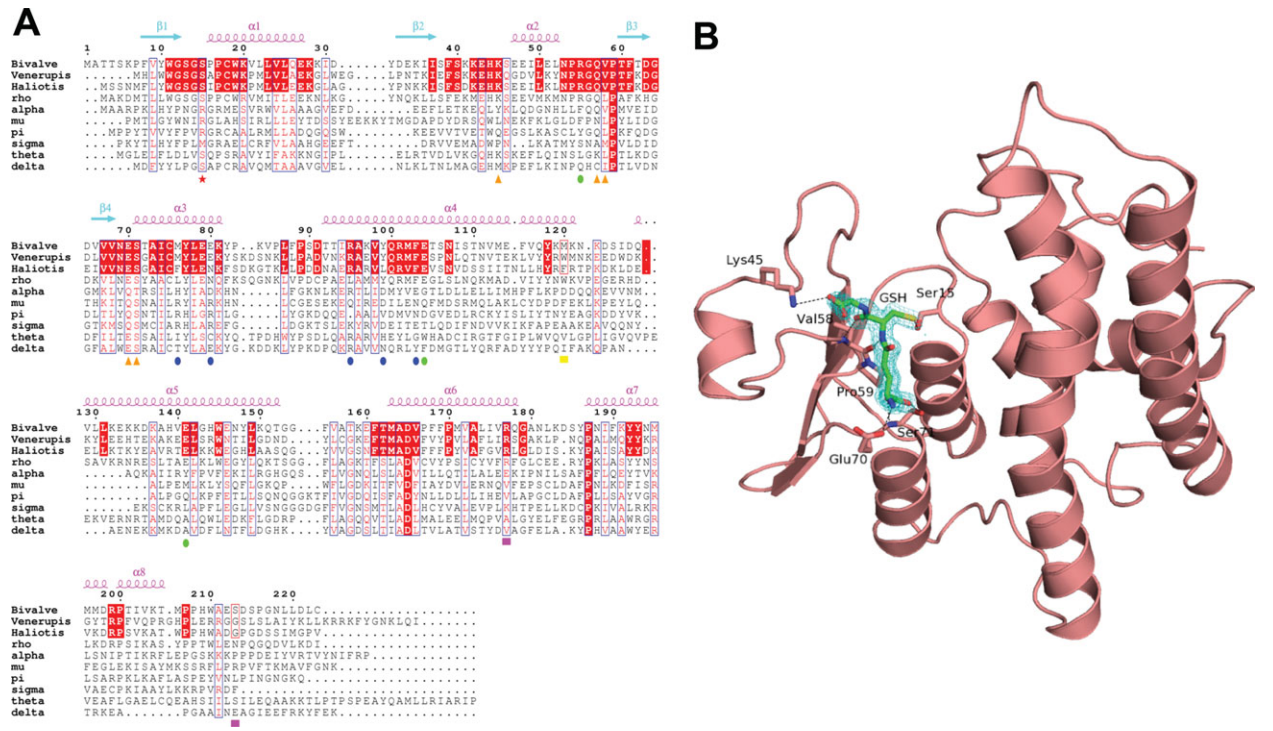

Figure 1

A: Sequence alignment of LeGST with two shellfish GSTs and other classes of GST. Secondary structure elements of LeGST are labeled above the sequence. The Ser residue, which forms a hydrogen bond with GSH is indicated by a red star. Residues that participate in GSH binding are indicated by orange triangles. The residues that participate in the dimer interactions through the hydrophobic cluster and salt-bridges are indicated by blue and green circles, respectively. The yellow square indicates the Met120 residue, which is expected to provide a hydrophobic environment for the H-site from the α4 helix. The Arg177 and Ser214 residues, which form the interaction between α6 and C-terminal tail, are indicated as pink squares. Amino acid sequences are as follows: Bivalve, LeGST; Venerupis, GST from *V. philippinarum*; Haliotis, GST from *H. discus discus*; rho, rho class GST of *P. major*; alpha, alpha class GST of Human; mu, mu class GST of human, pi, pi class GST of human, sigma, sigma class GST of squid; theta, theta class GST of human; delta, delta class GST of insect. B. Overall structure of LeGST. Residues involved in the GSH interaction and bound GSH are presented as a stick model and colored as salmon and green, respectively. The electron density map of GSH is also shown. The map was calculated with $(2|F_o|-|F_c|)$ and contoured at 1.5σ.

previous reports [Fig. 1(A)]. In a recent report, LeGST was grouped into the rho class of the GST family.[9] LeGST has ~40 % sequence identity with the rho class of the GST family, but there are no clearly established criteria concerning the extent of sequence similarity required for placing a GST in a particular class. It is generally accepted that GSTs within a class typically share greater than 40% identity and those between classes share less than 25% identity.[7] Therefore, it is difficult to conclusively state that LeGST belongs to the rho class GST based only on sequence identity (Supporting Information Fig. S1).

As previously mentioned, there are several unique features of LeGST that may warrant reclassification into a new GST class. First, the substrate specificity of LeGST is different from that of rho class GSTs. The rho class GST demonstrated a narrow range of substrate specificity and relatively low catalytic efficiency when compared to other classes of GSTs. On the other hand, LeGST displayed activity toward the substrate CDNB, 4-chloro-7-nitro-2,1,3-benzoxadiazole (NBD-Cl), ethacrynic acid (ECA), and 4-nitrophenyl acetate (4-NPA).[9] These results imply that the substrate spectrum of LeGST is broader than rho class GSTs. Moreover, when the specific activity of LeGST toward CDNB was compared with that of the rho class GST, the LeGST had a relatively high activity when compared to the rho class GST (2-fold higher). Another unique feature is observed in the three-dimensional structure of LeGST. Although LeGST had low sequence identity with other known structures, it adopted the canonical GST fold [Fig. 1(B)].

Active site

GSTs have two discrete ligand binding sites per monomer: a glutathione-binding site (G-site) and a pocket, in which the hydrophobic substrates bind (H-site). The G-site is similar in all structures and the overall geometry of the G-site is well-conserved in LeGST. At the beginning of β3, the *cis* Pro59 plays an important role in the

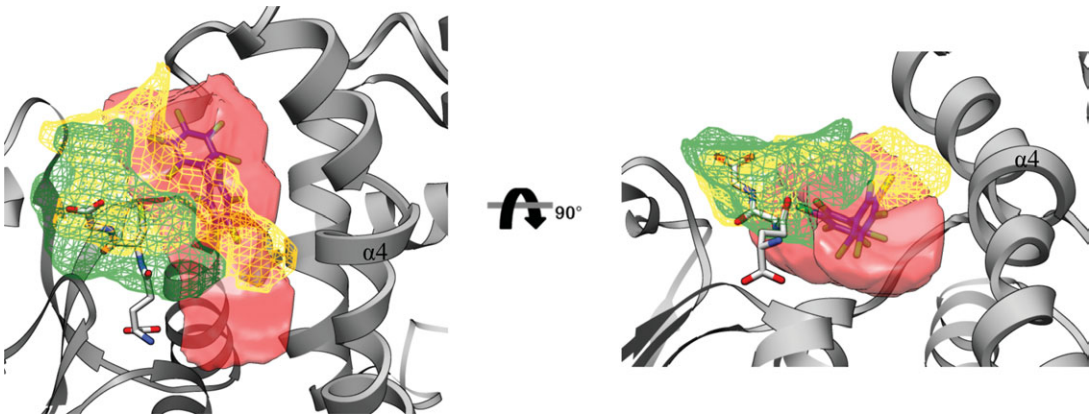

Figure 2

Comparison of the volume of H-site in LeGST (red as surface model), pi class GST (yellow as mesh), and PfGST (green as mesh). The bound model of PCB to the H-site of LeGST was calculated by AutoDock Vina[29] and manually docked using COOT.[20] The H-site volume was calculated by 3V[30] and the figure was generated using UCSF Chimera.[31] The GSH was excluded in the calculation and the outer and inner probe radiuses were set to 8 and 2, respectively. The only α4 helix is marked in the figure.

formation of turn, which is crucial for glutathione binding, and the most conserved core ββα motif, which is essential for the recognition of the γ-glutamyl component of the glutathione, is formed. The two residues (corresponding to Glu70 and Ser71 in LeGST) that are located in the turn between β4 and α3 are involved in these interactions. In LeGST, the γ-glutamyl moiety of glutathione interacts with the OE1 atom from Glu70 and the OG1 atom of Ser71, and the glycyl moiety interacts with the NZ atom from Lys45. The carbonyl oxygen and nitrogen atom of Val58 and the main chain carbon atom of Gln57 interact with the backbone of the cysteinyl moiety of the glutathione [Fig. 1(B)]. Unlike the tyrosine residue, which is a common catalytic residue of GSTs, the cysteinyl moiety of LeGST formed a hydrogen bond with a serine residue, as was observed for the theta and delta class GST.

The H-site of LeGST reveals more variation, which allows the GSTs to react with a wide variety of hydrophobic substrates. The H-site is covered with three sides in almost all GST families. The first loop between β1 and α1 makes the floor of the H-site, and α4 forms the sides or walls of the cavity, and the ceiling of the H-site is formed by an external C-terminal tail. Usually, the hydrophobic side chains are positioned in the α4 helix and C-terminal tail, which stabilizes the hydrophobic substrates by optimizing the hydrophobic environment. That is, the substrate recognition at the H-site is primarily mediated by hydrophobic interactions.

The structural analysis of the LeGST showed that there were several candidate hydrophobic residues in the α4 helix that could form an H-site. Among them, there are two aromatic residues, Tyr118 and Phe115. Tyr118 is a completely conserved residue in all shellfish GSTs. However, the crystal structure of LeGST showed that both Tyr118 and Phe115 could not form parallel stacking interactions with hydrophobic substrates since these residues were orientated in the opposite direction of the H-site. In contrast, Met120, which is an equivalent hydrophobic residue in shellfish GSTs (Trp and Phe in *V. philippinarum* and *H. discus,*[22] respectively), is orientated toward the H-site. However, Met120 is far from the H-site (more than 4.5 Å) when compared with those of other class GSTs because of its kinked α4 helix. For one of these three residues to participate in substrate binding at the H-site, the α4 helix would need to undergo a large conformational change to reduce the space between the H-site and hydrophobic residue. There were no remarkable conformational changes in the α4 helix upon binding to hydrophobic substrates when the native and inhibitor complex structure of other GSTs were compared with each other. Therefore, these findings suggest that Met120 participates in the hydrophobic interaction, which results in a larger and wider H-site (Supporting Information Fig. S2A).

In addition, the other hydrophobic interactions were usually provided by the C-terminal tail in other GST classes, but the long C-terminal tail of LeGST was not able to participate in the formation of the H-site due to point toward the C-terminal domain. The long C-terminal tail interacts with the C-terminal domain, especially the α4, α5, and α6 helix, through hydrogen bonds. Among them, hydrogen-bonding between Arg177, which is a completely conserved residue in all shellfish GST, and Ser213, which corresponds to the Gly residue in *V. philippinarum* and *H. discus* GSTs,[22] allow the C-terminal tail to be in direct contact with the C-terminal domain (Supporting Information Fig. S2B).

Both of the kinked α4 helix and long C-terminal tail contribute to an open and wide H-site of LeGST. From

the volume calculation of the H-site, LeGST was 739.9 Å^3, and the alpha, pi class GST, and GST from *Plasmodium falciparum* (PfGST)[23–25] were 190 Å^3, 367.9 Å^3, and 344.4 Å^3, respectively. It clearly shows that the H-site of LeGST forms a relatively large and wide active site compared to others, and it is also possible to accommodate the PCB molecule in its H-site, since the volume of the PCB molecule is ~420 Å^3. In other words, the relatively bulky and deep pocket shape of the H-site in LeGST is sufficient to accommodate the fully chlorinated PCB molecules and all four of its substrates, which are composed of aromatic ring compounds (Fig. 2).

Dimer interaction

There are two main factors of LeGST that contribute to dimer formation and one is the hydrophobic cluster formed around the two-fold axis (Supporting Information Fig. S3A). The inter-subunit interactions of LeGST are formed by the two α-helices, α3 and α4 helix from the symmetric equivalent subunit, which forms a bundle around a two-fold axis. Around the two-fold axis, the four residues (Met76, Tyr99, Met102, and Phe103) interact with their symmetric equivalent residues across the interface. These residues make a hydrophobic cluster similar to the zeta class GST from *Arabidopsis thaliana* (AtGST),[26] and two salt-bridges between Glu80 and Arg95 are formed in LeGST. In addition to these salt-bridges, hydrogen bonds between Glu80 and Tyr99 are formed at the base of the interface (Supporting Information Fig. S3B). Hydrogen bonds have also been observed in AtGST and it is suggested that this bond prevents LeGST and AtGST from forming heterodimers with GSTs of other classes.[26]

The second unique feature that contributes to the dimer interaction is the three salt-bridges, which is only observed in LeGST. In alpha, pi class GSTs and PfGST, there is a lock-and-key motif at the inter-subunit interface that is also dominated by hydrophobic interactions. The superposition of the LeGST structure with alpha, pi class of GSTs and PfGST indicates that the three salt-bridges are present in a similar position to the lock-and-key motif (Supporting Information Fig. S3C). The Arg55 on the α2-β3 loop acts as a key and Glu104 from α4 and Glu141 from α5 in the other subunit act as a lock in the modified lock-and-key motif.

The modified lock-and-key motif of LeGST was clearly defined when compared with other GST structures, such as the epsilon class of GST (PDB ID : 2IL3)[27] and Gtt2 from *Saccharomyces cerevisiae* (PDB ID : 3IBH, ScGtt2)[28] (Supporting Information Fig. S3D). In the epsilon class of GST, an interaction between Gln52 and Thr144 is observed. In ScGtt2, there are two interactions between each subunit (Asn67-Arg119 and Ser69-Glu123). In contrast, the Arg55 of LeGST is embedded in the lock motif, which is made by Glu104 and Glu141. This conformational feature is not observed in the above two GSTs. Also, the number of helices that participate in the hydrogen interactions is different. In LeGST, the two alpha helices (α4 and α5) forms the lock motif that is similar to the hydrophobic lock-and-key motif; however, in the epsilon class GST and ScGtt2, only one alpha helix (α5 and α4, respectively) participates in the hydrogen bonding interaction. Consequently, the modified lock-and-key motif may be one attribute that could be used to separate LeGST from other classes of GSTs.

Protein data bank accession code

The atomic coordinates and structure factors of native and GSH complex structures have been deposited in the Protein Data Bank, http://www.rcsb.org/pdb (PDB ID codes: 3QAV and 3AQW).

ACKNOWLEDGMENTS

The authors thank the staff at beamline 4A and 6C of Pohang Light Source, South Korea for assistance during data collection.

REFERENCES

1. Chasseaud LF. The role of glutathione and glutathione-*S*-transferases in the metabolism of chemical carcinogens and other electrophilic agents. Adv Cancer Res 1979;29:175–274.
2. Kettere B, Coles B, Meyer DJ. The role of glutathione in detoxification. Environ Health Perspect 1983;49:59–69.
3. Willett K, Wilson C, Thomsen J, Potter W. Evidence for and against the presence of polynuclear aromatic hydrocarbon and 2,3,7,8-tetrachloro-*p*-dioxin binding proteins in the marine mussels, *Bathymodiolus* and *Modiolus modiolus*. Aquat Toxicol 2000;48:51–64.
4. Salinas AE, Wong MG. Glutathione *S*-transferases—a review. Curr Med Chem 1999;6:279–309.
5. Strange RC, Spiteri MA, Ramachandran S, Fryer AA. Glutathione-*S*-transferase family of enzymes. Mutat Res 2001;482:21–26.
6. Wilce MC, Parker MW. Structure and function of glutathione *S*-transferases. Biochim Biophys Acta 1994;1205:1–18.
7. Hayes JD, Flanagan JU, Jowsey IR. Glutathione transferases. Annu Rev Pharmacol Toxicol 2005;45:51–88.
8. Konish T, Kato K, Araki T, Shirakis K, Takagi M, Tamaru Y. A new class of glutathione *S*-transferase from the hepatopancreas of the red sea bream *Pagrus major*. Biochem J 2005;388:299–307.
9. Park H, Ahn IY, Kim H, Lee J, Shin SC. Glutathione *S*-transferase as biomarker in the Antartic bivalve *Laternula elliptica* after exposure to the polychlorinated biphenyl mixture Aroclor 1254. Comp Biochem Physiol C-Toxicol Pharmacol 2009;150:528–536.
10. Ahn IY, Lee SH, Kim KT, Shim JH, Kim DY. Baseline heavy metal concentrations in the Antarctic clam, *Laternula elliptica* in Maxwell Bay, King George Island, Antarctica. Mar Pollut Bull 1996;32:592–598.
11. Stien X, Percic P, Gnassia-Barelli M, Roméo M, Lafaurie M. Evaluation of biomarkers in caged fishes and mussels to assess the quality of waters in a bay of the NW Mediterranean Sea. Environ Pollut 1998:99:339–345.
12. Goldberg ED, Bertine KK. Beyond the Mussel Watch—new directions for monitoring marine pollution. Sci Total Environ 2000:247:165–174.
13. Le Pennec G, Le Pennec M. Induction of glutathione-*S*-transferases in primary cultured digestive gland acini from the mollusk bivalve

Pecten maximus (L.): application of a new cellular model in biomonitoring studies. Aquat Toxicol 2003:64:131–142.
14. Boutet I, Tanguy A, Moraga D. Characterization and expression of four mRNA sequences encoding glutathione *S*-transferases pi, mu, omega and sigma classes in the Pacific oyster *Crassostrea gigas* exposed to hydrocarbons and pesticides. Mar Biol 2004:146:53–64.
15. Hoarau P, Damiens G, Roméo M, Gnassia-Barelli M, Bebianno MJ. Cloning and expression of a GST-pi gene in *Mytilus galloprovincialis*. Attempt to use the GST-pi transcript as a biomarker of pollution. Comp Biochem Physiol C Toxicol Pharmacol 2006:143:196–203.
16. Blanchette B, Feng X, Singh BR. Marine glutathione *S*-transferases. Mar Biotechnol 2007;9:513–542.
17. Jang EH, Park H, Park AK, Moon JH, Chi YM, Ahn IY. Crystallization and preliminary X-ray crystallographic studies of the ρ-class glutathione *S*-transferase from the Antarctic clam *Laternula elliptica*. Acta Crystallogr Sect F 2008;64:1132–1134.
18. Otwenowsky Z, Minor W. Processing of X-ray diffraction data collected in oscillation mode. Methods Enzymol 1997;276:307–326.
19. Zwart PH, Afonine PV, Grosse-Kunstleve RW, Hung LW, Ioerger TR, McCoy AJ, McKee E, Moriarty NW, Read RJ, Sacchettini JC, Sauter NK, Storoni LC, Terwilliger TC, Adams PD. Automated structure solution with the PHENIX suite. Methods Mol Biol 2008;426:419–435.
20. Emsley P, Cowtan K. Coot: model-building tools for molecular graphics. Acta Crystallogr Sect D 2004;60:2126–2132.
21. Laskowski RA, Moss DS. Main-chain bond lengths and bond angles in protein structures. J Mol Biol 1993;231:1049–1067.
22. Benson DA, Karsch-Mizrachi I, Lipman DJ, Ostell J, Sayers EW. GenBank. Nucleic Acids Res 2010;38:46–51.
23. Cameron AD, Sinning I, L'Hermite G, Olin B, Board PG, Mannervik B, Jones TA. Structural analysis of human alpha-class glutathione transferase Al-1 in the apo-form and in complexes with ethacrynic acid and its glutathione conjugate. Structure 1995;15: 717–727.
24. Oakley AJ, Rossjohn J, Lo Bello M, Caccuri AM, Federici G, Parker MW. The three-dimensional structure of the human Pi class glutathione transferase P1-1 in complex with the inhibitor ethacrynic acid and its glutathione conjugate. Biochemistry 1997;36:576–585.
25. Hiller N, Fritz-Wolf K, Deponte M, Wende W, Zimmermann H, Becker ,K. Plasmodium falciparum glutathione *S*-transferase--Structural and mechanistic studies on ligand binding and enzyme inhibition. Protein Sci 2006;15:281–289.
26. Thom R, Dixon DP, Edwards R, Cole DJ, Lapthorn AJ. The structure of a zeta class glutathione *S*-transferase from *Arabidopsis thaliana*: characterisation of a GST with novel active-site architecture and a putative role in tyrosine catabolism. J Mol Biol 2001;308:949–962.
27. PDB ID: 2IL3.Wang Y, Qui L, Ranson H. Lumjuan N, Hemingway J, Setzer WN, Meehan EJ, Chen J. "Structure of an insect epsilon class glutathione *S*-transferase from the malaria vector *Anopheles gambiae* provides an explanation for the high DDT-detoxification activity. J Struct Biol 2008;164:228–235.
28. PDB ID: 3IBH.Ma XX, Jiang YL, He YX, Bao R, Chen YX, Zhou CZ. Structures of yeast glutathione *S*-transferase Gtt2 reveal a new catalytic type of GST family. Embo Rep 2009;10:1320–1326.
29. Trott O, Olson AJ. AutoDock Vina: improving the speed and accuracy of docking with a new scoring function, efficient optimization, and multithreading. J Comput Chem 2009;31:455–461.
30. Voss NR. Gerstein M. 3V: cavity, channel and cleft volume calculator and extractor. Nucleic Acids Res 2010;38:555–562.
31. Pettersen EF, Goddard TD, Huang CC, Couch GS, Greenblatt DM, Meng EC, Ferrin TE. UCSF Chimera—a visualization system for exploratory research and analysis. J. Comput Chem 2004;25: 1605–1612.